The 2D and 3D Compounds $[M_2bpm(dca)_4]\cdot nH_2O$ (M = Ni, Zn; bpm = bipyrimidine; dca = dicyanamide; n = 0, 1) − Structural Analysis and Magnetic Properties

Susana Martín,[a] M. Gotzone Barandika,[a] Roberto Cortés,*[a] J. I. Ruiz de Larramendi,[a] M. Karmele Urtiaga,[b] Luis Lezama,[c] M. Isabel Arriortua,[b] and Teófilo Rojo*[c]

Keywords: Magnetic properties / Structure elucidation / N ligands / Nickel / Zinc

The combined use of bpm (2,2′-bipyrimidine) and dca (dicyanamide) has led to the preparation of two compounds of general formula $[M_2bpm(dca)_4]\cdot nH_2O$. Compound **1** (M = Ni, n = 1) exhibits a 2D layered structure based on ladder-like moieties. These units, whose steps are bpm groups, extend through single dca bridges, the connection between distinct ladder-like units taking place through double dca bridges. Compound **2** (M = Zn, n = 0) consists of a 3D structure based on the same type of ladder-like moieties that are connected to another four on the plane perpendicular to the extension of the ladders.

Introduction

The design of multidimensional networks has been an important area of research in coordination chemistry. Thus, the preparation of crystalline materials exhibiting some desired structural and topological features becomes a fascinating challenge as it implies the control of the related physical and chemical properties. In this sense, the synthetic strategy has been widely confirmed to be a major factor.

Among the variety of extended frameworks reported during the last few years, there are plenty of examples that illustrate the relevance of the synthetic strategy. Since the azide pseudohalide has been one of the most used ligands, a couple of azide systems can be mentioned in this context (Scheme 1). For instance, the compound $[Mn(N_3)_2bpy]_n$ (bpy = 2,2′-bipyridine) consists of Mn chains where the Mn^{II} ions are alternatively bridged by double *end-on* (EO) and double *end-to-end* (EE) azide bridges.[1] The substitution of bpy by the tetradentate bpm (2,2′-bipyrimidine) in an M:bpm molar ratio of 2:1 induces the connection of the Mn chains resulting in the compound $[Mn_2(N_3)_4bpm]_n$. This is a 2D honeycomb-like structure where the sheets exhibit an infinite hexagonal array of Mn^{II} ions bridged by bis-chelating bpm and double EO azide-bridges.[2]

A further step in the synthetic strategy could consist of the substitution of the azide group to generate new M-bpm-L compounds (L being the new ligand). With this aim, we have selected dicyanamide (dca), as previously done by other researchers.[3] This ligand, similarly to the azide li-

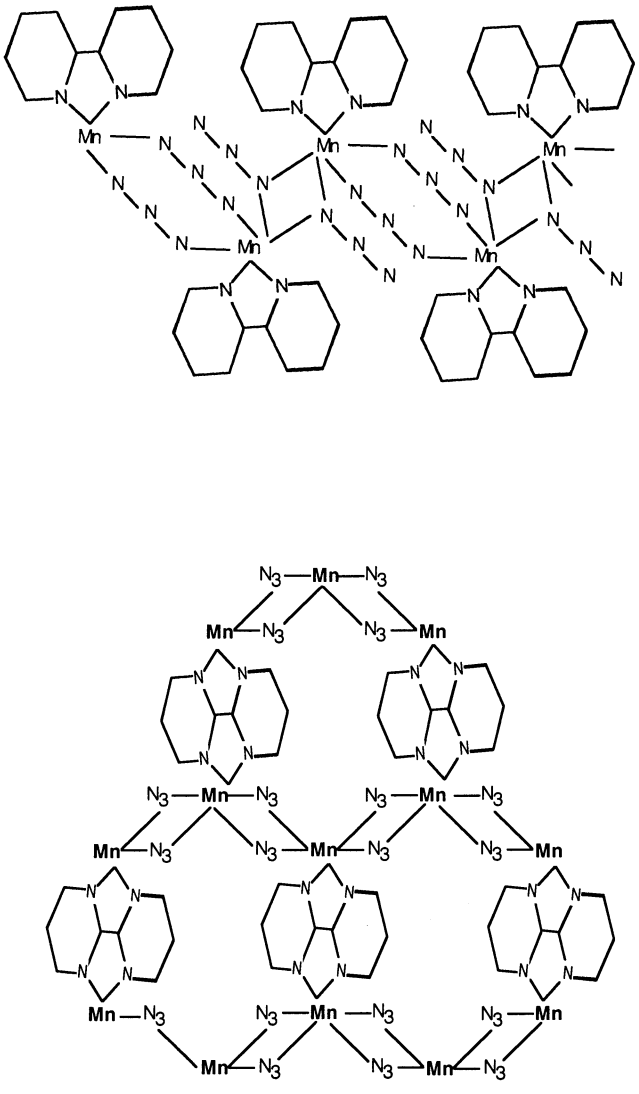

Scheme 1

[a] Departamento de Química Inorgánica, Facultad de Farmacia, Universidad del País Vasco,
Apdo. 450, Vitoria 01080, Spain
[b] Departamento de Mineralogía-Petrología, Facultad de Ciencias, Universidad del País Vasco,
Apdo. 644, Bilbao 48080, Spain
[c] Departamento de Química Inorgánica, Facultad de Ciencias, Universidad del País Vasco,
Apdo. 644, Bilbao 48080, Spain
E-mail: qiproapt@lg.ehu.es

  1434−1948/01/0808−2107 $ 17.50+.50/0

gand, exhibits several coordination modes. Thus, besides the monodentate terminal coordination,[4] bidentate,[5] tridentate[6] and even tetradentate[7] modes have been reported for dca (Scheme 2). The potential of dca for the preparation of extended frameworks is illustrated by the great deal of recent attention focussed on coordination polymers containing this ligand.[8]

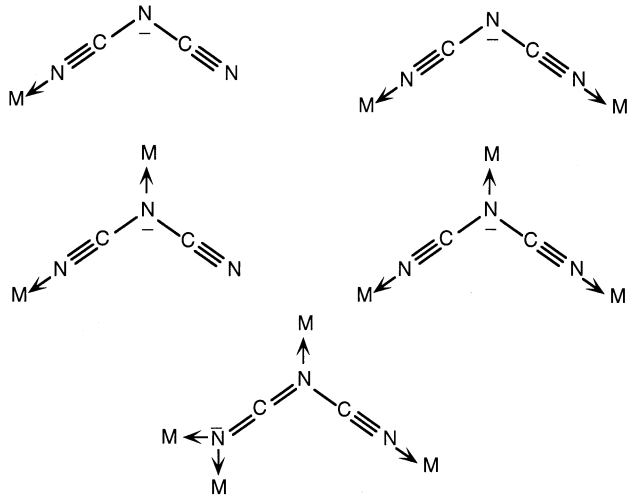

Scheme 2

Taking into account the above-mentioned aspects, two compounds of general formula $[M_2bpm(dca)_4]\cdot nH_2O$ (M = Ni, $n = 1$ for compound **1**; M = Zn, $n = 0$ for compound **2**) have been synthesised and magnetostructurally characterised. For both of them, a ladder-like moiety can be proposed as a basic structural unit whose repetition leads to a 2D array for **1** and to a 3D network for **2**.

Results and Discussion

Structural Analysis

The structural characterisation of compound **1** has been carried out by means of X-ray powder-diffraction pattern analysis on the basis of the structure of $[Co_2bpm(dca)_4]\cdot H_2O$ (**3**). This compound has been structurally characterised at 100 K by Marshall et al.[3] and at 273 K by us. Therefore, since the X-ray powder-diffraction data collection for **1** was carried out at 273 K, we have used our structural data for **3** as initial parameters for the refinement of **1**. The observed, calculated and difference X-ray diffraction pattern for **1** are displayed in Figure 1. As can readily be seen, there is a good agreement between the theoretical and experimental data. Thus, the fact that **1** and **3** exhibit the same stoichiometry and space group (*Pnma*) and similar structural parameters [a = 16.111(3) Å, b = 12.755(2) Å, c = 10.455(2) Å for **1** and a = 16.212(2) Å, b = 12.972(2) Å, c = 10.502(2) Å for **3**] clearly indicates that compounds **1** and **3** are isomorphous. This isomorphous relationship is also confirmed by the rest of the analytical techniques discussed in this work for **1**.

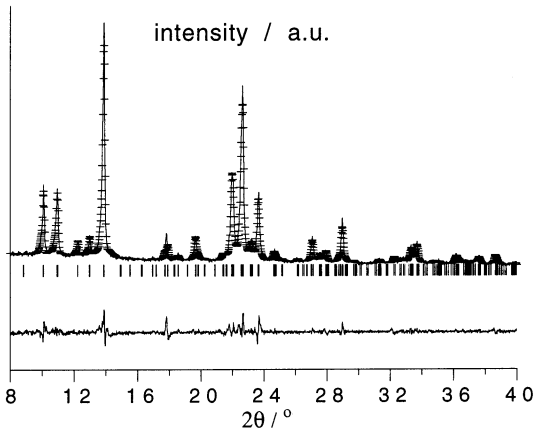

Figure 1. Observed, calculated and difference X-ray diffraction patterns for **1**

Figure 2 shows a view of the structures of **1** and **3**. As observed, they consist of layers of octahedrally coordinated metallic cations. The 2D network can be described on the basis of ladder-like moieties extending along the x direction through single dca bridges, the steps being the bpm groups. These ladders are connected through double dca bridges along the y direction. The intermetallic distance through bpm is the shortest one (5.770 Å for **3**) while the distance through the single dca bridges is the longest one (8.299 Å for **3**), with the one through double dca links being intermediate (7.202 Å for **3**). The layers are waved and are closely packed along the z direction. Additionally, there are molecules of water of crystallisation located between these layers.

Compound **2** consists of a 3D network where each Zn^{II} cation is octahedrally bonded to one bpm (through N1 and N2 atoms) and four dca ligands (two N3−C5−N4−C6−N5 groups and two N6−C7−N7−C8−N8 groups). As seen in Figure 3, the two N_{bpm} atoms occupy two of the equatorial positions. Since the bpm ligands are N,N',N'',N'''-tetradentate they allow the connection between two metallic cations. On the other hand, the four dca groups act as 1,5-bridges with the N3 and N6 atoms at the remaining equatorial positions and the N5 and N8 atoms at the axial positions. As a result each Zn^{II} cation is linked to five metallic centres: one through bpm (Zn···Zn distance is 5.895 Å) and four by dca ligands [Zn···Zn distances through the N3,N5- and N6,N8-bonded dca groups are 7.446 and 7.656 Å, respectively].

The 3D structure of **2** can also be described on the basis of covalently interconnected ladder-like moieties. Thus, as observed in Figure 4, the ladder-like moieties also consist of bpm steps. These units extend along the x direction through N3−C5−N4−C6−N5 dca groups. Each ladder unit is connected to another four through N6−C7−N7−C8−N8 dca groups along the [011] and [$\bar{0}$1] directions.

Table 1 displays the selected bond lengths and angles for **2**. As can be seen, the coordination sphere is quite distorted in relation to both distances and angles. The presence of the rigid bpm ligand accounts for the bond angles being far from the ideal values. The Zn−N8 distance deserves special

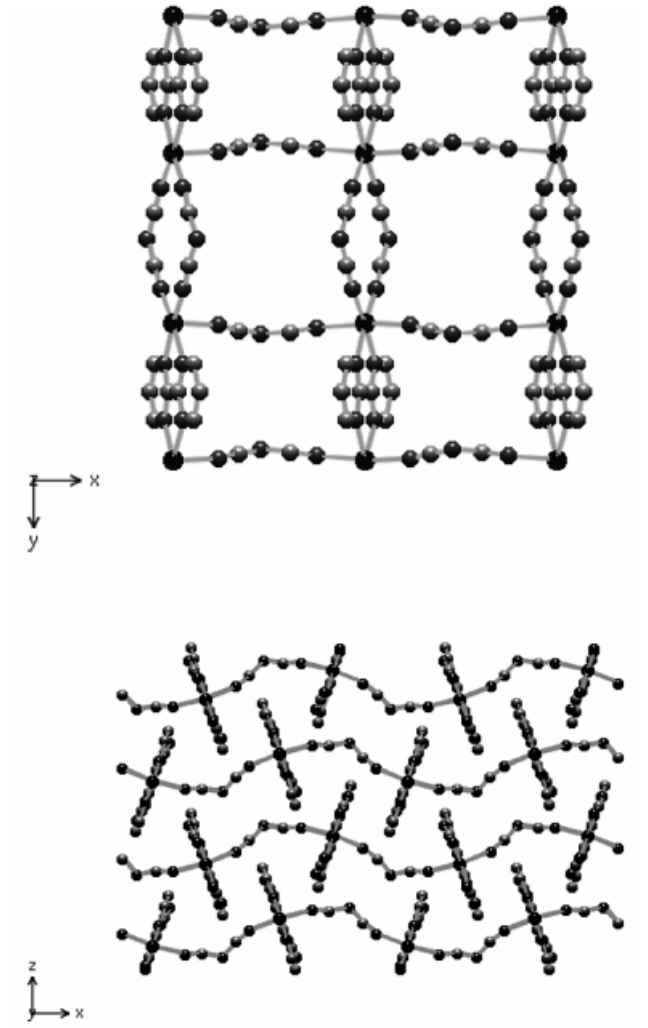

Figure 2. (top) View of the 2D structure and (bottom) the packing of the layers for **1**

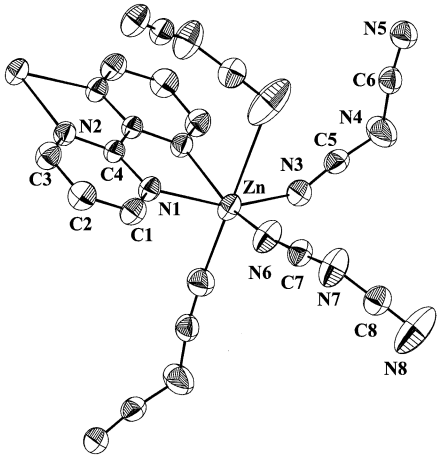

Figure 3. ORTEP view (50% probability) of the coordination environment for **2**

attention as the value of 2.8 Å clearly implies that the covalent connection between distinct ladder-like units is weak. Nevertheless, similar values have been accepted in the literature as bond lengths.[9]

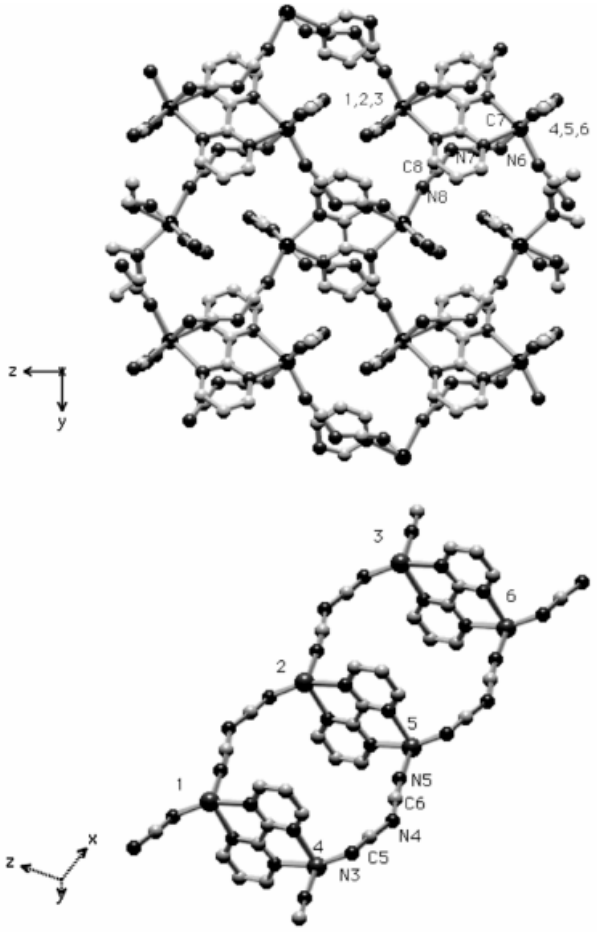

Figure 4. (Top) [011] view of the structure for **2** and (bottom) extension of the ladder-like moieties along the [100] direction

Table 1. Selected bond lengths (Å) and angles (°) for compound **2**[a]

Zn−N(1)	2.171(2)	N(5)−Zn−N(2i)	98.67(8)
Zn−N(2i)	2.258(2)	N(6)−Zn−N(3)	100.31(10)
Zn−N(3)	2.028(2)	N(6)−Zn−N(1)	92.84(8)
Zn−N(5)	2.030(2)	N(3)−Zn−N(1)	158.51(8)
Zn−N(8)	2.788(2)	N(6)−Zn−N(2i)	157.67(8)
Zn−N(6)	2.040(2)	N(3)−Zn−N(2i)	87.44(8)
N(3)−C(5)	1.149(3)	N(1)−Zn−N(2i)	74.42(6)
C(5)−N(4)	1.285(3)	C(5)−N(3)−Zn	142.07(18)
N(4)−C(6)	1.294(3)	N(3)−C(5)−N(4)	172.7(3)
C(6)−N(5ii)	1.146(3)	C(5)−N(4)−C(6)	123.5(2)
N(6)−C(7)	1.137(3)	N(5ii)−C(6)−N(4)	171.7(3)
C(7)−N(7)	1.295(3)	C(6iii)−N(5)−Zn	171.8(2)
N(7)−C(8)	1.292(3)	C(7)−N(6)−Zn	163.1(2)
C(8)−N(8)	1.127(4)	N(6)−C(7)−N(7)	172.6(3)
N(5)−Zn−N(6)	100.49(10)	C(8)−N(7)−C(7)	122.1(2)
N(5)−Zn−N(3)	100.08(9)	N(8)−C(8)−N(7)	172.8(3)
N(5)−Zn−N(1)	94.08(8)		

[a] Symmetry transformations used to generate equivalent atoms: i = $-x$, $-y$, $-z$; ii = $x-1$, y, z; iii = $x+1$, y, z.

The main difference between the structures for **1** and **2** lies in the connection between ladder-like units. Thus, while each ladder is connected to another two through double dca bridges along the *y* direction for **1**, each ladder is linked to another four through single dca bridges for **2**. This is a

consequence of the orientation of the coordination octahedra in relation to the extension of the ladder-like moiety. Thus, for **1** the axial direction of the octahedra fully coincides with the extension direction, while for **2** it does not. Obviously, this different disposition is responsible for the occurrence of a 2D array for **1** and a 3D structure for **2**.

IR and ESR spectroscopy

A summary of the most important IR bands corresponding to compounds **1** and **2**, together with their tentative assignment,[10] is displayed in Table 2. As observed, both compounds exhibit strong absorptions in the region 2315−2190 cm^{-1} that correspond to $\nu_{C\equiv N}$ modes. There are also strong bands at about 1580 cm^{-1} for both of them (with a shoulder at lower wavenumbers for **2**) that have been attributed[11] to the asymmetric doublet characteristic of ring stretching for bis-chelating bpm. The absorptions due to molecules of water of crystallisation were detected for **1** at about 3400 cm^{-1}.

Table 2. IR bands (cm^{-1}) and assignments for compounds **1** and **2**

	1	**2**
dca, ν_{sym} + ν_{asym} (C≡N)	2312i	2352i,2292i
dca, ν_{asym} (C≡N)	2257i	2265i
dca, ν_{sym} (C≡N)	2190i	2225i, 2165i
dca, ν (C−N)	1413m, 1360m	1415i, 1360i
bpm, (C=C, C=N), bis-chelating	1585m	1580i, 1565i
H_2O, crystallisation (O−H)	3410m	−

An X-band ESR spectrum at room temp. was recorded on a powdered sample of **2** doped with 1 mol % Cu (Figure 5). As observed, the signal is characteristic of an axial *g* tensor exhibiting hyperfine splitting on the parallel component which corresponds to the electronic spin−nuclear spin (^{67}Cu, $I = 3/2$) coupling. Values of $g_{\|} = 2.315$, $g_{\perp} = 2.075$ and $A_{\|} = 143 \times 10-4\,cm^{-1}$ have been determined. The sequence $g_{\|} > g_{\perp} > 2.04$ indicates a $d_{x^2-y^2}$ ground state in good agreement with the elongated octahedral topology of the $[CuN_6]$ chromophores.[12]

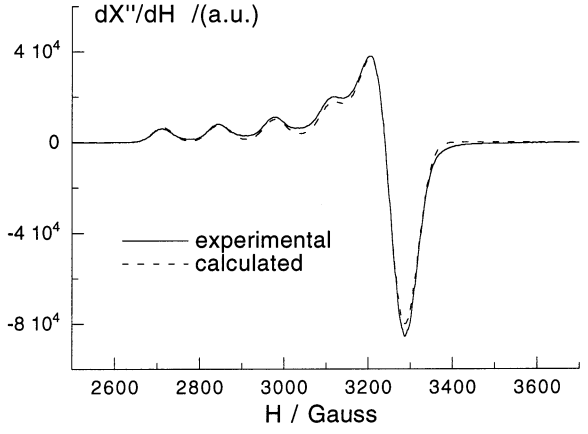

Figure 5. Experimental and calculated ESR powder spectra for $[(Zn_{0.99}Cu_{0.01})_2bpm(dca)_4]$

Magnetic Properties

The magnetic characterisation of compound **1** was carried out by measurement of the thermal variation of the magnetic susceptibility, χ_m. The experimental data, plotted as the thermal variation of the reciprocal susceptibility (χ_m^{-1}) and the product $\chi_m T$ are shown in Figure 6.

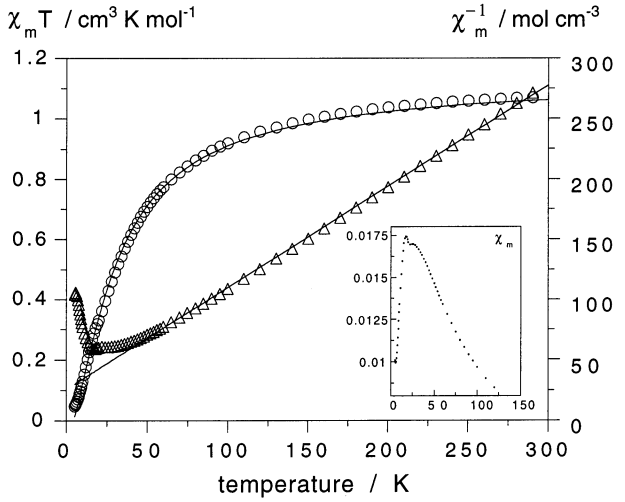

Figure 6. Thermal evolution of χ_m^{-1} and $\chi_m T$ for **1** and their corresponding theoretical curves (fit 2 for $\chi_m T$)

The χ_m values for **1** increase from 3.53×10^{-3} cm^3 mol^{-1} at room temp. up to a maximum, and afterwards decrease, tending to zero. The peak in χ_m shows two maxima (16.54×10^{-3} cm^3 mol^{-1} at 24 K and 16.95×10^{-3} cm^3 mol^{-1} at 17 K). This small anomaly, shown in the inset in Figure 6, will be discussed below. The Curie−Weiss law is followed down to 50 K with values of $C_m = 1.19$ cm^3 K mol^{-1} and $\theta = -30.75$ K. The $\chi_m T$ curve decreases continuously upon cooling from 1.07 cm^3 K mol^{-1} (per Ni atom) at room temp., tending to zero.

The magnetic results for **1** are clearly indicative of the occurrence of antiferromagnetic coupling between metallic centres. Since the dca ligand is a poor magnetic mediator,[13] these interactions should be attributed mainly to the exchange through the bpm ligand.[3,14]

In order to evaluate the antiferromagnetic interactions for **1**, Equation (1) was used first. This expression, based on the isotropic spin Hamiltonian $H = -JS_A \cdot S_B$, accounts for the molar magnetic susceptibility corresponding to a Ni^{II} dimer ($S_A = S_B = 1$).

$$\chi_m = \frac{2N\beta^2 g^2}{kT}\left[\frac{\exp(J/kT) + 5\exp(3J/kT)}{1 + 3\exp(J/kT) + 5\exp(3J/kT)}\right] \quad (1)$$

where *N* and *k* are the Avogadro and Boltzmann constants, respectively, and β is the Bohr magneton.

This model reproduces the experimental data quite accurately with values of $J = -18.3$ cm^{-1} and $g = 2.12$ (fit 1). However, as mentioned above, there is a small anomaly on the χ_m vs. *T* curve for **1** that has not been explained. This anomaly could be attributed to the occurrence of weak ex-

change through the dca bridges at low temperatures that could provoke a slight lack of compensation of the antiparallel spins. If we now consider this exchange as an interdimer molecular field,[3] the magnetic data for **1** can be interpreted by Equation (2). The best theoretical curve generated (fit 2) is displayed in Figure 6 ($J = -16.5$ cm^{-1}, $g = 2.14$ and $zJ' = -3.1$ cm^{-1}). It is worth mentioning that no significant improvement has been found compared to fit 1.

$$\chi = \frac{\chi_m}{\left(1 - \frac{2k}{Ng^2\beta^2} zJ' \chi_m\right)} \quad (2)$$

The sign and magnitude of the exchange constants J calculated for the interaction through bpm is comparable to others found in the literature. Thus, values between -14 and -11 cm^{-1} have been reported for Ni-bpm-Ni bridges.[15] The moderate efficiency of bis-chelating bpm as a magnetic coupler is explained by the strong overlap between $d_{x^2-y^2}$ magnetic orbitals (the x and y axes being the ones corresponding to the $Ni-N_{bpm}$ bonds) through the symmetry-adapted HOMO of the bpm bridge.[16] The fact that the Ni-bpm-Ni fragment is practically planar favours the overlap increasing the magnitude of the coupling.

The isomorphous Co^{II} compound (**3**) has been characterised magnetically by Marshall et al.[3] Compound **3** exhibits antiferromagnetic interactions that are mainly attributed by the authors to the dimeric exchange through bpm (as found for **1**). Unfortunately, since the attempts by Marshall et al. to model the magnetic behaviour of **3** do not lead to any J values, there is no possible comparison between the exchange constants for **1** and **3**.

Conclusion

The combined use of dca and bpm has led to the preparation of extended frameworks with two Ni^{II} and Zn^{II} atoms. The antiferromagnetic Ni^{II} compound exhibits a 2D array where ladder-like units are connected through double dca bridges. The bpm ligands are the steps in the ladder-like moieties, their extension taking place through single dca bridges. Molecules of water of crystallisation can be found between the resulting waved planes. The Zn^{II} compound is anhydrous and exhibits the same kind of ladder-like units. In this case, however, each unit is connected to another four through single dca bridges resulting in a 3D array.

Experimental Section

Synthesis: The synthesis of compound **1** was carried out by mixing an aqueous solution of $Ni(NO_3)_2\cdot 6H_20$ (0.50 mmol) and a methanolic solution of bpm (0.25 mmol). Afterwards, an aqueous solution of dca (1 mmol) was added and left to stand at room temperature. After several days, poor-quality blue crystals were obtained (45% yield, 62.57 mg). Unfortunately, further attempts to recrystallise this product did not lead to better quality crystals. The synthesis of compound **2** was performed in a similar manner with $ZnCl_2$. In this case, prismatic, yellow, X-ray quality single crystals (34% yield, 62.22 mg) were obtained.

Elemental analysis and atomic absorption results were in good agreement with the $C_8H_3N_8NiO_{0.5}$ stoichiometry for **1**, and the $C_8H_3N_8Zn$ stoichiometry for **2**.
1: calcd. C 34.4, H 1.4, N 40.2, Ni 21.0; found C 33.0, H 1.7, N 38.3, Ni 21.2.
2: calcd. C 34.7, H 1.1, N 40.5, Zn 23.6; found C 34.5, H 1.0, N 39.3, Zn 23.1.

Physical Measurements: Microanalyses were performed with a LECO CHNS-932 analyser. Analytical measurements were carried out in an ARL 3410 + ICP with a Minitorch equipment. IR spectroscopy was performed on a Nicolet 520 FTIR spectrophotometer in the 400−4000 cm^{-1} region. ESR spectroscopy was performed on powdered samples at the X-band frequency, with a Bruker ESR 300 spectrometer equipped with a standard OXFORD low-temperature device, which was calibrated by the NMR probe for the magnetic field. The frequency was measured with a Hewlett−Packard 5352B microwave frequency computer. Magnetic susceptibilities and the magnetisation of powdered samples were carried out in the temperature range 1.8−300 K at values of the magnetic field up to 10000 G, using a Quantum Design Squid magnetometer, equipped with a helium continuous-flow cryostat. The experimental susceptibilities were corrected for the diamagnetism of the constituent atoms (Pascal tables).

Crystal Structure Determination: X-ray powder diffraction data for compound **1** were collected on a PHILIPS X′PERT powder diffractometer with Cu-K_α radiation in steps of 0.02° (2θ) over the 5−60° (2θ) angular range and a fixed-time counting of 4 seconds at 25 °C. The powder diffraction patterns were indexed with the FULLPROF[16] program based on the Rietveld method[17−18]using the *Profile Matching* option. Crystallographic data and processing parameters for compound **1** are given in Table 3.

Table 3. Crystallographic data for **1**

Formula	$C_8H_3N_8NiO_{0.5}$
M	278.11
Crystal system	Orthorhombic
Space group	*Pnma*
a [Å]	16.111(3)
b [Å]	12.755(2)
c [Å]	10.455(2)
α [°]	90
β [°]	90
γ [°]	90
U [Å^3]	2148.4
Z	8
T [K]	293
λ [Å]	1.5425
R_p[a]	7.50
R_{wp}[b]	9.80
GOF[c]	2.55

[a] $R_p = 100[100(|y_o - y_c|)/|y_o|]$. − [b] $R_{wp} = [(w|y_o - y_c|^2)/(w|y_o|^2)]^{1/2}$. − [c] GOF $= [R_{wp}/R_{expected}]^2$.

X-ray measurements for **2** were carried out at room temperature on an Enraf−Nonius CAD-4 diffractometer operating in the ω/2θ scanning mode. Accurate lattice parameters were determined from a least-squares refinement of 25 well-centred reflections. Intensity data were collected in the θ range 1−30°. During data collection, two standard reflections observed periodically showed no signific-

ant variation. Corrections for Lorentz and polarisation factors were applied to the intensity values. The structure for **2** was solved by heavy-atoms Patterson methods using the program SHELXS-97[19] and refined by a full-matrix least-squares procedure on F^2 using SHELXL-97.[20] Non-hydrogen atomic scattering factors were taken from International Tables of X-ray Crystallography.[21] Crystallographic data and processing parameters for **2** are shown in Table 4.

Crystallographic data (excluding structure factors) for the structure(s) included in this paper have been deposited with the Cambridge Crystallographic Data Centre as supplementary publication no. CCDC-150936 (**2**) and -150937 (**3**). Copies of the data can be obtained free of charge on application to CCDC, 12 Union Road, Cambridge CB2 1EZ, UK [Fax: (internat.) + 44-1223/336-033; Email: deposit@ccdc.cam.ac.uk].

Table 4. Crystal data and structure refinement for compound **2**

Formula	$C_8H_3N_8Zn$
M	276.55
Crystal system	Monoclinic
Space group	$P2_1/c$
a [Å]	7.446(4)
b [Å]	11.478(4)
c [Å]	12.064(4)
α [°]	90
β [°]	107.75(2)
γ [°]	90
U [Å^3]	982.0(7)
Z	4
T [K]	293
λ [Å][a]	0.71069
ρ_{obs} [g cm^{-3}]	1.85(4)
ρ_{cal} [g cm^{-3}]	1.871
μ [mm^{-1}]	2.489
Unique data	2860
Observed data	2299
$R(R')$[b]	0.0356(0.1031)

[a] Graphite monochromated Mo-K_α radiation. – [b] $R = [||F_o| - |F_c||/|F_o|]$, $R' = \{[w(F_o^2 - F_c^2)^2]/[w(F_o^2)^2]\}^{1/2}$, where $w = 1/\sigma^2\gamma|F_o|$.

Acknowledgments

This work has been carried out with the financial support of the Universidad del País Vasco/Euskal Herriko Unibertsitatea (Grant UPV 130310-EB201/1998), Gobierno Vasco/Eusko Jaurlaritza (Project 99/53) and the Ministerio de Educación y Cultura (Project PB97–0637). S. M also thanks the Gobierno Vasco/Eusko Jaurlaritza for the doctoral fellowship associated to the project PI96/39.

[1] R. Cortés, M. Drillon, X. Solans, L. Lezama, T. Rojo, *Inorg. Chem.* **1997**, *36*, 677–683.
[2] [2a] R. Cortés, L. Lezama, J. L. Pizarro, M. I. Arriortua, T. Rojo, *Angew. Chem. Int. Ed. Engl.* **1996**, *35*, 1810–1812. – [2b] R. Cortés, M. K. Urtiaga, L. Lezama, J. L. Pizarro, M. I. Arriortua, T. Rojo, *Inorg. Chem.* **1997**, *36*, 5016–5021.
[3] S. R. Marshall, C. D. Incarvito, J. L. Manson, A. L. Rheinhold, J. S. Miller, *Inorg. Chem.* **2000**, *39*, 1969–1973.
[4] [4a] I. Potocnák, M. Dunaj-Jurco, D. Miklos, L. Jäger, *Acta Crystallogr., Sect. C* **1996**, *52*, 1653–1655. – [4b] I. Potocnák, M. Dunaj-Jurco, D. Miklos, M. Kabesová, L. Jäger, *Acta Crystallogr., Sect. C* **1995**, *51*, 600–602.
[5] [5a] Y. M. Chow, *Inorg. Chem.* **1971**, *10*, 1938–1942. – [5b] Y. M. Chow, D. Britton, *Acta Crystallogr., Sect. C* **1977**, *33*, 697–699. – [5c] D. Britton, *Acta Crystallogr., Sect. C* **1990**, *46*, 2297–2299. – [5d] J. L. Manson, C. D. Incarvito, A. L Rheinhold, J. S. Miller, *J. Chem. Soc., Dalton Trans.* **1998**, 3705–3706. – [5e] J. Mrozinski, M. Hvastijová, J. Kohout, *Polyhedron* **1991**, *11*, 2867–2871.
[6] J. L. Manson, C. R. Kmety, Q. Huang, J. W. Lynn, G. Bendele, S. Pagola, P. W. Stephens, L. M. Liable-Sands, A. L. Rheingold, A. J. Epstein, J. S. Miller, *Chem. Mater.* **1998**, *10*, 2552–2560.
[7] Y. M. Chow, D. Britton, *Acta Crystallogr., Sect. C* **1975**, *31*, 1934–1936.
[8] [8a] S. R. Batten, P. Jensen, B. Moubaraki, K. S. Murray, R. Robson, *Chem. Commun.* **1998**, 439–440. – [8b] J. L. Manson, D. W. Lee, A. L. Rheingold, J. S. Miller, *Inorg. Chem.* **1998**, *37*, 5966–5967. – [8c] J. L. Manson, C. R. Kmety, A. J. Epstein, J. S. Miller, *Inorg. Chem.* **1999**, *38*, 2552–2553. – [8d] P. Jensen, S. R. Batten, G. D. Fallon, B. Moubaraki, K. S. Murray, D. J. Price, *Chem. Commun.* **1999**, 177–178. – [8e] S. R. Batten, P. Jensen, C. J. Kepert, M. Kurmoo, B. Moubaraki, K. S. Murray, D. J. Price, *J. Chem. Soc., Dalton Trans.* **1999**, 2987–2997. – [8f] P. Jensen, S. R. Batten, G. D. Fallon, D. C. R. Hockless, B. Moubaraki, K. S. Murray, R. Robson, *J. Solid State Chem.* **1999**, *145*, 387–393. – [8g] J. L. Manson, A. M. Arif, J. S. Miller, *J. Mat. Chem.* **1999**, *9*, 979–983. – [8h] P. Jensen, S. R. Batten, B. Moubaraki, K. S. Murray, *Chem. Commun.* **2000**, 793–794. – [8i] A. Escuer, F. A. Mautner, N. Sanz, R. Vicente, *Inorg. Chem.* **2000**, *39*, 1668–1673.
[9] [9a] A. Bino, N. Cohen, *Inorg. Chim. Acta* **1992**, *210*, 11–17. – [9b] D. K. Lavallee, A. B. Kovelove, O. P. Anderson, *J. Am. Chem. Soc.* **1978**, *100*, 3025–3033.
[10] K. Nakamoto, *Infrared Spectra of Inorganic and Coordination Compounds*, John Willey & Sons, New York, **1997**.
[11] [11a] F. Berezovsky, A. A. Hajem, S. Triki, J. S. Pala, P. Molinie, *Inorg. Chim. Acta* **1999**, *248*, 8–13. – [11b] G. De Munno, M. Julve, F. Lloret, J. Faus, A. J. Caneschi, *J. Chem. Soc., Dalton Trans.* **1994**, 1175–1183.
[12] J. A. Weil, J. R. Bolton, E. Wertz, *Electron Spin Resonance, Elementary Theory and Practical Applications*, 2nd Ed., John Wiley & Sons, New York, **1994**.
[13] J. L. Manson, A. M. Arif, C. D. Incarvito, L. M. Liable-Sands, A. L. Rheingold, J. S. Miller, *J. Solid State Chem.* **1999**, *145*, 369–378.
[14] G. De Munno, G. Viau, M. Julve, F. Lloret, J. Faus, *Inorg. Chim. Acta* **1997**, *257*, 121–129.
[15] [15a] G. De Munno, M. Julve, F. Lloret, A. Derory, *J. Chem. Soc., Dalton Trans.* **1992**, 1179. – [15b] G. Brewer, E. Sinn, *Inorg. Chem.* **1985**, *24*, 4580–4585.
[16] M Julve, G. De Munno, G. Bruno, M. Verdaguer, *Inorg. Chem.* **1988**, *27*, 3160–3165.
[17] J. Rodriguez-Carvajal, FULLPROF, *Program for Rietveld Pattern Matching Analysis of Powder Patterns*, **1997**.
[18] H. M. Rietveld, *Acta Crystallogr.* **1967**, *12*, 151–152.
[19] H. M. Rietveld, *J. Appl. Cryst.* **1969**, *6*, 65–67.
[20] G. M. Sheldrick, SHELXS-97. Program for the Solution of Crystal Structures. University of Göttingen, Germany, **1997**.
[21] G. M. Sheldrick, SHELXL-97. Program for the Refinement of Crystal Structures. University of Göttingen, Germany, **1997**.
[22] *International Tables for X-ray Crystallography, Vol. IV*, Kynoch Press, Birmingham, U.K, **1974**.

Received January 19, 2001
[I01036]